ESCUELA DE CONSTRUCCIÓN CIVIL
FACULTAD DE INGENIERÍA

Revista de la Construcción
Journal of Construction

Research Article

Numerical investigation of the lateral load behavior of core and coupled rocking walls

Shokrullah Sorosh[1], **Ali Sari**[2*]

[1] Department of Civil Engineering, Istanbul Technical University, Istanbul (Turkey), sorosh@itu.edu.tr
[2] Department of Civil Engineering, Istanbul Technical University, Istanbul (Turkey), asari@itu.edu.tr
*Correspondence: asari@itu.edu.tr

Received: 28.08.2021; **Accepted:** 9.04.2022; **Published:** 18.04.2022

Citation: Sorosh, S. and Sari, A. (2022). Numerical investigation of the lateral load behavior of core and coupled rocking walls. Revista de la Construcción. Journal of Construction, 21(1), 36-52. https://doi.org/10.7764/RDLC.21.1.36.

Abstract: During last few decades, the researchers have developed new structural systems which have no or minor damage after being hit by severe events like earthquake. Development of self-centering wall having alternative energy dissipation mechanisms was one of these achievements. A wide variety of rocking wall systems, such as jointed walls, hybrid walls, precast walls with end columns (PreWEC), and PreWEC core wall systems, are proposed and studied. This paper describes an analytical investigation of the lateral load behavior of two new types of hybrid rocking wall systems. Core rocking wall is achieved by merging four single hybrid rocking walls and coupled rocking wall is accomplished by coupling two rocking walls using embedded reinforced concrete beams. The concept of coupling hybrid rocking walls using embedded reinforced coupling beam is emerged from previous coupled conventional shear walls studies. As single rocking wall system, in coupled and core rocking wall, post-tensioning tendons are used as a mean to provide self-centering force, and mild steel bars are used to dissipate energy. The nonlinear behavior of the wall is due to the gap opening at the base joint. Three-dimensional finite element model of each system was developed. The stress distribution, crack propagation, and critical sections of these systems are investigated. The effect of spalling concrete cover in the toe region due to rocking action is explained. In addition, the reduction in stiffness and lateral load resisting capacity of the systems due to cracks is monitored. Finally, the lateral load behavior of single rocking walls is compared to that of core and coupled rocking wall systems.

Keywords: rocking wall, reinforced concrete structures, coupled rocking wall system, core rocking wall system, finite element analysis.

1. Introduction

Reinforced concrete walls, having high in plan stiffness, are providing an effective means to resist lateral and to limit the lateral deflection. Investigating the historical earthquake events, structural walls showed superior seismic performance than other structural components (Fintel, 1995). Vayas, Dasiou, and Marinelli (2007) cited by Henry (2011) is stating that although researchers have been studying the rocking behavior of structural components for the last six decades, the evidence shows its origin goes back to Greek era. For the first time, Housner (1963) studied the rocking behavior during investigation of the tall slender structures exposed to 1960 Chilean earthquake.

Retrofitting the piers of Lions Gate Bridge in Vancouver Canada was one of the early applications of rocking mechanism (Crippen, 2002). Aslam, Goddon, and Scalise (1980) during the investigation of rocking-behavior of massive concrete blocks

found out that rocking can be enhanced against overturning either by anchoring the blocks to the ground or allowing it to slide. Since this system dissipate minor energy, Stone, Cheok, and Stanton (1995) investigated the effect of mild steel bars as energy dissipation mean in hybrid systems. A seismic design methodology for unbonded pre-tensioned precast walls was introduced by Kurama, Sause, Pessiki, Lu, and El-Sheikh (1998). Later, Kurama, Sause, Pessiki, and Lu (1999) used the fiber-base model to simulate the hysteretic response of rocking walls utilizing DRAIN-2DX (Prakash & Powell, 1993).

Due to insubstantial research in precast concrete area, the application of precast components was limited. To solve this restriction, in the early 1990's, a joint US-Japan research program called PRESSS (Precast Seismic Structural Systems) was established (Priestley, 1991). Several frame, wall, and floor diaphragm technologies developed in this research program were utilized in 60% scale prototype building test. One of the successes of this test was to introduce and study the lateral load behavior of jointed wall systems (Priestley, Sritharan, Conley, & Pampanin, 1999). In addition, this research program motivated researcher to conduct the idea of hybrid beam-column connection for precast concrete walls. Since jointed wall systems have smaller moment resisting capacity, researchers in Iowa State University introduced precast wall with end columns (PreWEC) (Aaleti & Sritharan, 2011). Sritharan, Aaleti, Henry, Liu, and Tsai ((2015) developed a new seismic resisting system that contains PreWEC. To connect the self-centering wall to end columns, they used mild steel connectors, that are easily replaceable and cost effective. Henry, Sritharan, and Ingham (2016) studied the behavior of this system using finite element method.

Several computational techniques such as fiber base model (Kurama et al., 1999), lumped plasticity model (Henry, 2011), and solid element model (Henry, 2011) have been introduced by researchers. Henry (2011) developed a solid element model of PreWEC core wall system using ABAQUS (Dassault, 2011). He found that the lateral load capacity of the wall is increased by 20% when four PreWEC form a core. In addition, there is recent research on finite element and analytical modeling approaches to study the impact damping (Kalliontzis & Nazari, 2021). In this research, the lateral load behavior of coupled and core rocking wall systems is investigated. Previously Kurama and Shen (2004) have analytically studied the usage of precast concrete coupling beams to couple hybrid walls. They coupled the hybrid walls using post-tensioned precast coupling beams. However, in this study, the hybrid wall systems are coupled using embedded reinforced concrete beams. Besides, the lateral load performance of the core rocking walls system is studied. The rocking walls were designed following ASCE 7-16 (2017), ACI 318 (2011) and ACI ITG-5.2 (2009) design codes.

In these design codes, the drift limits under design and maximum loads are obtained using formulas based on linear-elastic effective stiffness models in which the nonlinear performance of the rocking wall systems are purely coming from the gap opening at the base joint. However, this study monitors the real behavior of rocking wall system and take the effects of concrete cracks into account. It is investigated that how important it is to consider the impacts of concrete cracks on the performance of these wall systems. Using ATENA (Červenka, Jendele, & Červenka, 2017), Displacement based pushover analysis was performed on three dimensional models of these systems. Lateral load performance, stress distribution and crack propagation of the rocking wall systems were evaluated. The reduction in lateral load bearing capacity of the system due to cracks and spalling of concrete cover in the toe region is monitored.

2. Building description

The plan view of the building in which the rocking wall system is considered as lateral load bearing system is shown in Figure 1. Height of each story is 3.2 m. Beams have 250 mm x 550 mm dimensions. Columns dimensions are 400 mm x 800 mm. The slab thickness is 150 mm. To calculate the design loads, for the first, second, and third floors the dead load is taken as 5.94 kN/m^2 and live load is taken as 3.5 kN/m^2. However, for the last floor 5.38 kN/m^2 and 2 kN/m^2 are considered as dead load and live load, respectively. The interior wall unit weight is taken as 3 kN/m^2. To satisfy the minimum requirement given in ACI ITG-5.2 (2009), the compressive strength of concrete is 40 MPa. The unit weight of concrete is taken as 25 kN/m^3. The yield strengths of non-energy dissipating (non-E.D.) and energy dissipating (E.D.) steel reinforcement are taken as 420 MPa, and 450 MPa, respectively (ASTM A 615, 2003).

In this study, since the lateral load behavior of only rocking wall systems is studied, the finite element model of the whole building is not developed. Since the seismic loads are required to design the rocking wall systems, the prototype building shown in Figure 1 is used to calculate the seismic loads. The lateral load resisting of the building in X direction is provided by W_1 rocking walls, and in Y-Direction is provided by W_2 rocking walls.

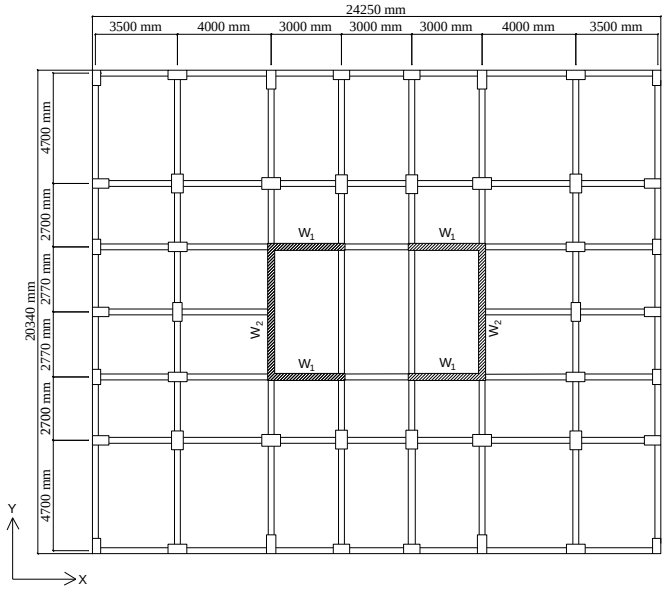

Figure 1. Plan view of the building.

Equivalent lateral load procedure, explained in ASCE 7-16 (2017), is used to calculate the lateral load forces. The design short period and 1.0 s spectral acceleration were 1 g and 0.64 g respectively. The total lateral force is obtained as 5000 kN. In design of rocking walls, the lateral load capacity of the frame is not considered. It is assumed that all walls in the same direction have equal rigidity and act as perfect rigid diaphragms. The design lateral load of W_1, W_2, and W_3 is calculated to be 1257.79 kN, 2529.51 kN, and 2506.31 kN respectively.

In this paper the finite element model of six rocking wall systems is developed. Two of which are W_1, and W_2 single rocking walls. W_3 is the rocking wall which has a total length of 9.2m and span the length between two W_2 walls. The fourth system is formed by coupling of two W_1 single rocking walls using embedded reinforced concrete beams. In the fifth system, two coupled systems are connected by two W_2 rocking walls. Finally, the sixth system is the core rocking wall system of two W_2 walls and two W_3 walls. Each of these systems is explained in detail in the next sections.

3. Design of rocking wall systems

ACI ITG-5.2 (2009), design guideline of special unbonded pre-tensioned precast shear walls and ACI 318 (2011), building code requirement for concrete structures are followed to design the rocking walls. In this paper the design procedures are not explained in detail. Hence, a more detail design procedure can be followed in a report prepared by Smith and Kurama (2012) at department of Civil Engineering and Geological Sciences at the University of Notre Dame. The design of all rocking walls follows two limit states: (1) Design drift limit (Δ_{wd}) in which the base of the wall is considered as fixed (ASCE 7-16, 2017). (2) Maximum drift limit (Δ_{wm}) in which the Eqs. (1) is followed ACI ITG-5.2 (2009). h_w, and l_w represent height and length of the wall, respectively.

$$0.95[0.9 \leq 0.8[h_w/l_w] + 0.5 \leq 3.0] \quad (1)$$

Since the E.D. bars and tendons are mostly placed near the center of the wall, in core and coupled rocking wall systems with end walls, it is strongly recommended to check the elongation of the E.D. reinforcements and tendons at the wall end under maximum drift level. Hence, in some conditions in which the wall drift results in fracture of E.D. bars or yielding of post-tensioning tendons (P.T), the maximum level drift should be lowered. In this case the maximum level drift is not following the Eqs. (1). The linear elastic drift (Δ_{we}) of the wall is obtained by assuming a cracked flexural stiffness of $I_{cr} = 0.5I_{gross}$ and shear area of $A_{sh} = 0.8A_{gross}$.

3.1. *W_1 rocking wall system*

The wall height (h_w) and length (l_w) are 14.8 m and 3.2 m respectively. The calculated drift limits were (Δ_{we}) = 0.278%, Δ_{wd} = 1.388 %, and Δ_{wm} = 1.9%. The design details of W_1 rocking wall conducted under two limit states is shown in Figure2. Considering the ACI ITG-5.2 (2009) and ACI 318 (2011), the base joint is designed in such a way that normal force and overturning moment are balanced by post-tensioning tendons and energy dissipating reinforcements. The eccentricity of bars and unbonded length are assumed and later by iteration the design is checked. For simplicity, in this study the P.T and E.D. bars are assumed as lumped bars. To assume bars as lumped, none of these bars should be placed beyond one quarter of the center of the wall. It is mentionable that the unbonded length of E.D. reinforcements are changing based on their eccentricity, but in lumped E.D. bars assumption the unbonded length of all E.D. reinforcements can be assumed to be equal. The strains of E.D. reinforcements and P.T are checked under maximum level drift. Since the E.D. bars are designed in such a way that they should yield to dissipate energy, the strain check is crucial. In addition, the self-centering forces of the system are provided by weight of the wall, dead loads and live loads carried by the wall, and normal forces developed in the tendons. Therefore, for the heavier rocking walls the PT is expected to be less than that of light weight walls. Upper joints and confinement zone in the toe region of the rocking walls are designed under maximum level drift and maximum lateral loads. Because no drift in upper joints is expected, the upper joints reinforcements should balance the forces developed in those joints and avoid the separation of the wall panel from each other. At the end, it is worthy of mentioning that the base of the rocking can also designed as curved as discussed in more detail in Lin, Wiebe, and Berman (2019).

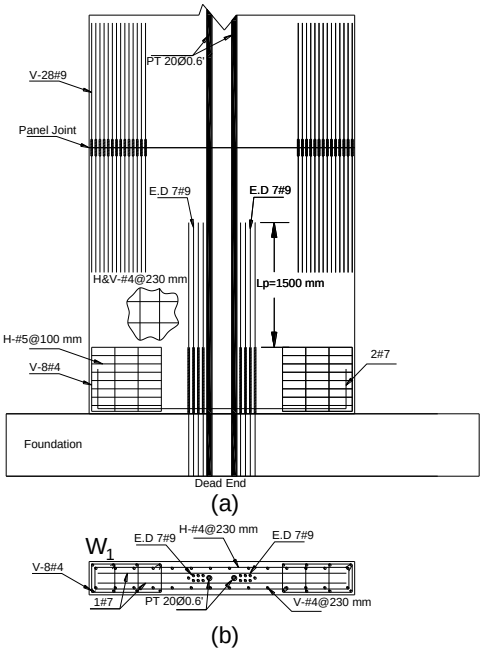

Figure 2. Reinforcement layout of W1 rocking wall: (a) elevation, (b) plan view.

3.2. *W_2 and W_3 rocking wall systems*

The W_2 wall height (h_w) and length (l_w) are 14.8 m and 6.28 m respectively. The calculated drift limits are (Δ_{we}) = 0.081%, Δ_{wd} = 0.407 %, and Δ_{wm} = 1.14%. The height of W_3 is the same as that of W_1, and W_2. The length of W_3 is 9.4 m. The drift limits for this system are (Δ_{we}) = 0.028%, Δ_{wd} = 0.139 %, and Δ_{wm} = 0.855%.The plan view of W_2 and W_3 rocking walls reinforcement details are shown in Figure 3 (a)-(b) respectively.

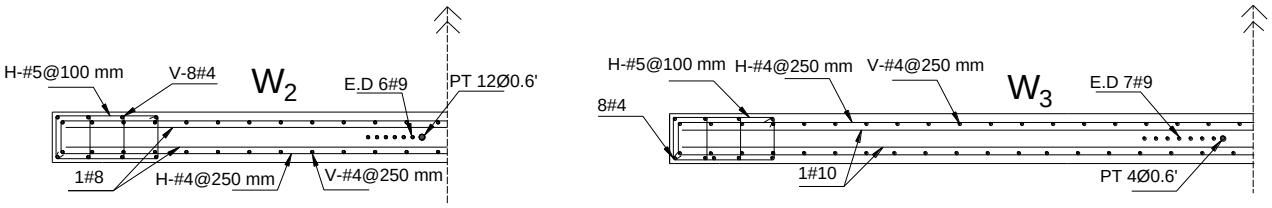

(a) (b)

Figure 3. Reinforcement schemes: (a) W2 plan view, (b) W3 plan view.

3.3. *Coupled rocking wall system*

Two W_1 rocking walls are coupled using embedded reinforced concrete beams. To design the coupling beams the internal forces under lateral load are determined using three-dimensional finite element model using SAP2000 software (CSI, 2018). The moment diagrams of beams are shown in Figure 4.

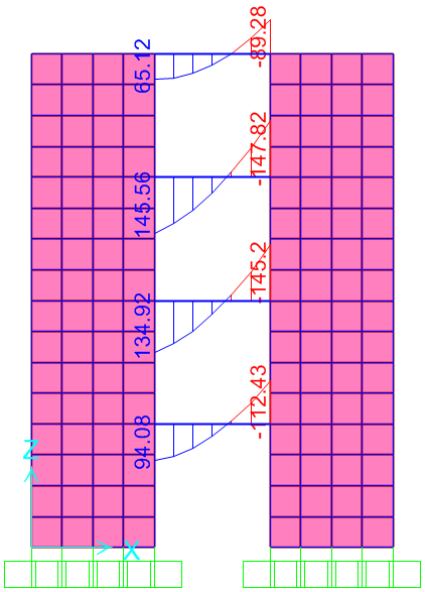

Figure 4. Moment diagrams of coupling beams.

Since the length to height ratio of coupling beam is larger than 4 and the design shear force is not exceeding the shear force limit, there is no need for diagonal reinforcements. The longitudinal reinforcement at the top and bottom section of the beam is required to be extended by 0.8 m development length inside the wall. In this study, there is no change in the reinforcement design of W_1 rocking walls after they are coupled. The aim of this action was to have a better comparison between the behavior of single wall and coupled walls. Figure 5 shows the reinforcement scheme of coupled rocking wall system.

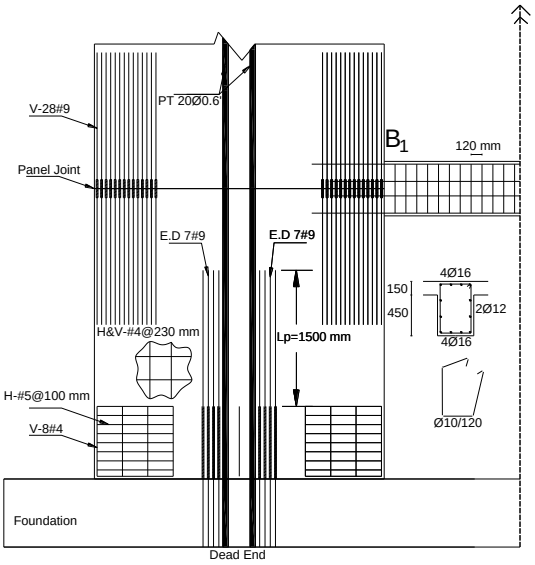

Figure 5. Elevation view of reinforcement scheme of coupled rocking wall system.

3.4. *Core rocking wall system*

Core rocking wall system is formed by two W_2, and two W_3 single rocking walls. There is no change in the reinforcement scheme of the W_2 and W_3 rocking walls. The plane view of the reinforcement details of this system is shown in Figure 6.

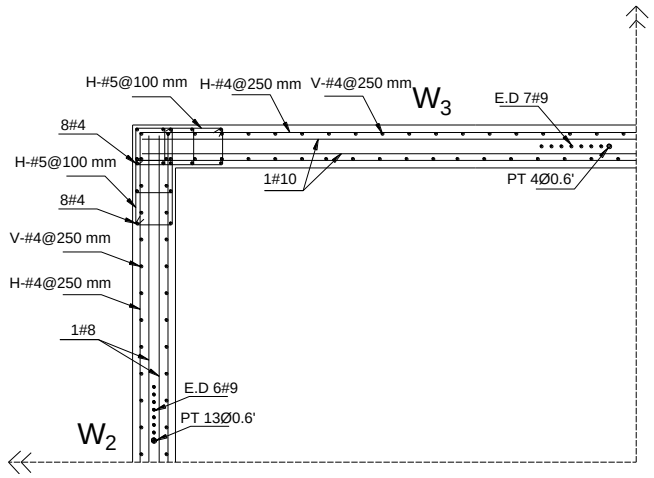

Figure 6. Plan view of reinforcement details for core rocking wall system.

4. Finite element model

Recently, one of the focuses of researchers has been the interaction between rocking walls and surrounding structural components such as beams and slabs. Henry (2011) studied this interaction by developing three-dimensional finite element model of the whole building using ABAQUS. He found out that under large lateral drifts, the relative displacement between surrounding structural components and rocking walls are large and, in some cases, this may damage the building seriously. Moroder, Sarti, Palermo, and Pampanin (2014) and Watkins, Sritharan, and Henry (2014) studied wall to floor connection using experimental approaches. Egidio, Pagliaro, Fabrizio, and Leo (2020) studied the seismic behavior of frame structure coupled with rocking wall. In this study, our main concern is not the interaction between wall to surrounding members. Hence,

the finite element models of only rocking wall systems are developed. Three-dimensional finite element models of the rocking wall systems are developed using ATENA software (Červenka et al, 2017). ATENA which stands for Advanced Tool for Engineering Nonlinear Analysis, is a software for nonlinear analysis of reinforced concrete structures. This software simulates the real behavior of concrete and reinforced concrete structures including concrete cracking, crushing and reinforcement yielding. In this study, the main aim of using the software was to check the reduction in stiffness and lateral load resisting capacity of the rocking wall system due to cracks as well as to capture the behavior of embedded reinforced concrete coupling beams.

Finite element modelling and analysis using ATENA have three steps which are pre-process, process, and post-process. In pre-process, the model is developed, and all input data are defined. In process step, the software is performing the required analysis. Finally, in post-process, the software is providing results of analysis. ATENA software can perform the process step of the models developed using GID (Červenka et al, 2017). GID is a pre- and post-processor for numerical simulations in science and engineering. In this study, while the pre-process is conducted using GID, the process and post-process are accomplished using ATENA software. All material libraries, boundary conditions, all required elements such as truss, beam, shell, and solid elements, as well the problem data required for the analysis in ATENA are existed in GID.

4.1. *Material properties*

Concrete is modelled using solid element having 40 MPa compressive design strength. The foundation and anchorage plates are modelled using rigid elastic material. The post-tensioning tendons are modelled using 1-D reinforcement bilinear material present in this software. The type of reinforcement is chosen as Tendon. Figure 7 shows the material model for tendons. In this figure, modulus of elasticity of tendons (E), Characteristic yielding strength (f_{xk}), maximum strain (ε_{uk}), and parameter k are taken as 190000 MPa, 1650 MPa, 0.02 and 1.09, respectively.

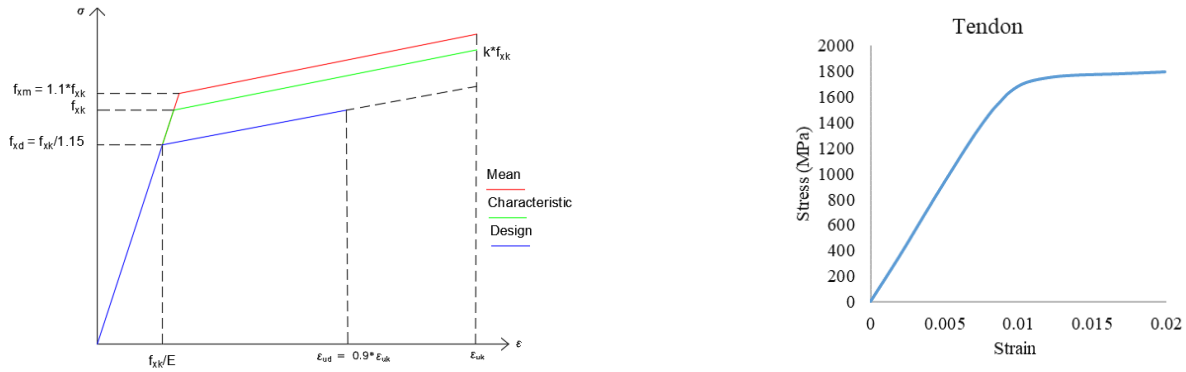

(a) (b)

Figure 7. Tendon stress-strain curve : (a) GID material model (Červenka et al, 2017) , (b) Real stress-strain curve (Smith & Kurama, 2012).

Tendons are unbounded throughout the wall height. The dead end of the tendon elements is fixed to the foundation and posttensioning stress is applied on the other end at the top of the wall. Taking the short term and long-term losses into account, the initial posttensioning stress is 55% of the characteristic yield strength of the tendons. Figure 8 shows the stress-strain relation of E.D. bars. To avoid stress concentration and fracture of bars, these bars are required to be unbonded over a specific length.

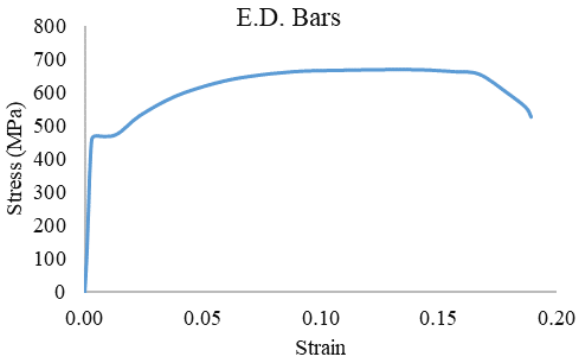

Figure 8. Stress-strain curve of E.D. bars (Smith & Kurama, 2012).

All other reinforcements are modelled using bilinear material model having 420 MPa characteristic yield strength. The gap at the base joint and rocking action are modelled in a wide variety of ways by researchers. For instance, Henry (2011) modelled the gap at the base joint using "Hard Contact" using ABAQUS. Hence, the sliding of the wall is prevented by "rough" friction.

In this research, a thin layer of 1 cm solid element is used to model the gap at the base joint. The material in thin layer has the same compressive strength as that of the concrete wall, but zero tensile strength. Hence, when the rocking action occurs, the loads are transferred safely to foundation. Besides, this thin layer shows zero tensile strength in lifting corner which results in gap opening in the form of crack.

4.2. *Pushover analysis*

Using ATENA software, the boundary conditions, prestressing forces, and other external forces are assigned in different interval data. Interval data include many steps which helps the user to converge the result. In this study, five interval data are used. The boundary conditions are defined in the first interval data. The contact between the wall panel and grout material, grout material and foundation are fixed type contacts. The weight and post-tensioning stresses are applied in the second and third interval data. In the next interval data, depending on the systems and convergence of the analysis result, small lateral displacement is applied to the wall end. In the last interval data, the displacement given in the fourth interval data is increased till the structure fails or specified lateral drift is reached.

5. Analysis results

5.1. *W_1 rocking wall system*

Considering the ACI ITG-5.2 (2009) and ACI 318 (2011), the design lateral load and drift under design load are defined. Using the overstrength factor, the maximum lateral load and corresponding drift were obtained in Section 3 of this paper. The lateral load-top displacement curves of the rocking wall systems obtained using finite element analysis are compared to the curves proposed by design codes. Moreover, previously studied by Henry (2011), the concrete in the toe region of rocking wall crashes due to rocking actions. To understand the effects of spalling of concrete at rocking toe region, three-dimensional finite model of the system without concrete cover at rocking toe region is developed. The stress distribution of W_1 rocking wall system considering both cases is shown in Figure 9 (a)-(b). In Figure 9(a), only cracks larger than 1 mm are shown. However, to understand the rocking action the cracks smaller than 1 mm in the rocking toe are shown. An excellent performance and well stress distribution of the wall are seen. Most of the cracks larger than 1 mm are concentrated in the wall panel near the base joint. Spacing of E.D. bars is one of the main reasons of these tensile cracks. Another fact to be considered, no confinement reinforcement is placed in this region. In conclusion, exceeding the unconfined concrete strength causes cracks in the elements. In Figure 9(b), the stress distribution of rocking wall without concrete cover at the toe region is shown. Comparing these two figures, it is well understood that stresses developed in the wall without concrete cover (See Figure 9(b)) is lower. This reduction in stress stems from reduction of lateral load capacity of wall.

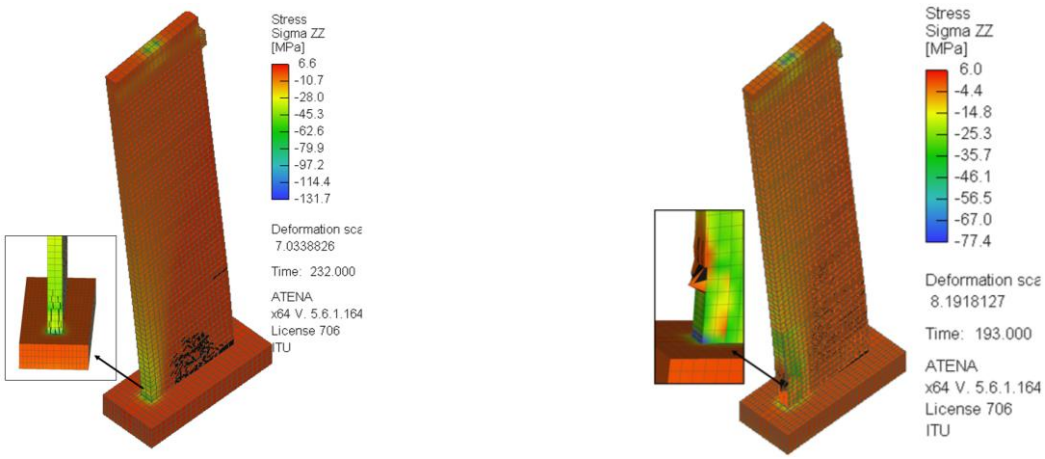

(a) (b)

Figure 9. Stress distribution of W1: (a) with concrete cover (b) without concrete cover.

The lateral load-top displacement relation of W_1 rocking wall system is displayed in Figure 10. In contrast to other analysis, finite element analysis of W_1 rocking wall shows higher rigidity and lateral load resisting strength than those of ACI curve. Because the length of W_1 wall is small and carry huge over-turning moment under maximum level drift, to avoid the gap opening in the upper joints a substantial amount of steel bars is needed. In this study, to satisfy this condition, 28#9 bars are placed in the first story joint which causes a stiffer wall. Furthermore, in this figure, the impact of concrete spalling is clearly monitored. The initial rigidity of the wall is not affected much by concrete spalling. However, after initial elastic drift is reached, the wall loses its rigidity, and the lateral load resisting strength of the system is decreased by approximately 10 %.

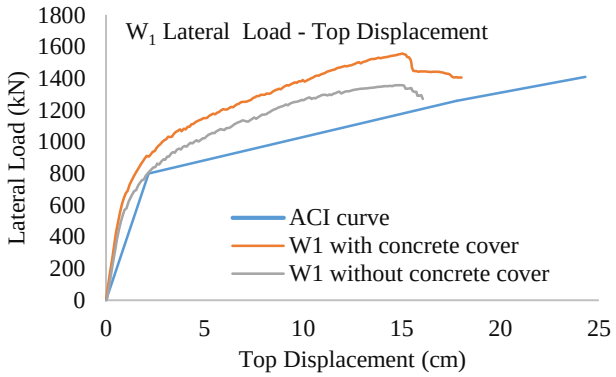

Figure 10. Lateral load-top displacement curve of W1 rocking wall system.

5.2. *W_2 and W_3 rocking wall systems*

The stress distribution of W_2 and W_3 rocking wall systems are shown in Figure 11 (a)-(b) respectively. These two systems also showed perfect performance and well distribution of stress. In rocking toe, the stress reaches 55 MPa. Like W_1 wall, most of the tensile cracks larger than 1 mm occur in the wall panel near the base. In these regions, due to wall lifting and gap opening, the E.D. bars develop tensile stress in concrete which causes cracking.

The lateral load-top displacement curve of W_2 and W_3 rocking wall systems are shown in Figure 12 and Figure 13 respectively. The behavior of W_2 wall under lateral loads are studied by considering two conditions. In the first case, the wall panel behaves elastically, and no crack occurs in the wall. In the second case, the real behavior concrete is taken into consideration. In ACI ITG-5.2 (2009) and ACI 318 (2011), only the flexural and shear deflections are considered in the lateral drift limit calculations, and the formulas used to obtain these drift limits are obtained from linear-elastic effective stiffness models. The

nonlinear behavior of the rocking walls is fully due to the gap opening at the base joint. Nevertheless, this study is considering the real performance of concrete and impacts of concrete cracks are not ignored. Therefore, as it is seen in Figure 12, the finite element analysis result of elastic wall approaches the ACI curve. The effects of concrete cracks on the lateral load resisting capacity as well as the maximum drift capacity of the wall can be seen clearly from Figure 12 and Figure 13.

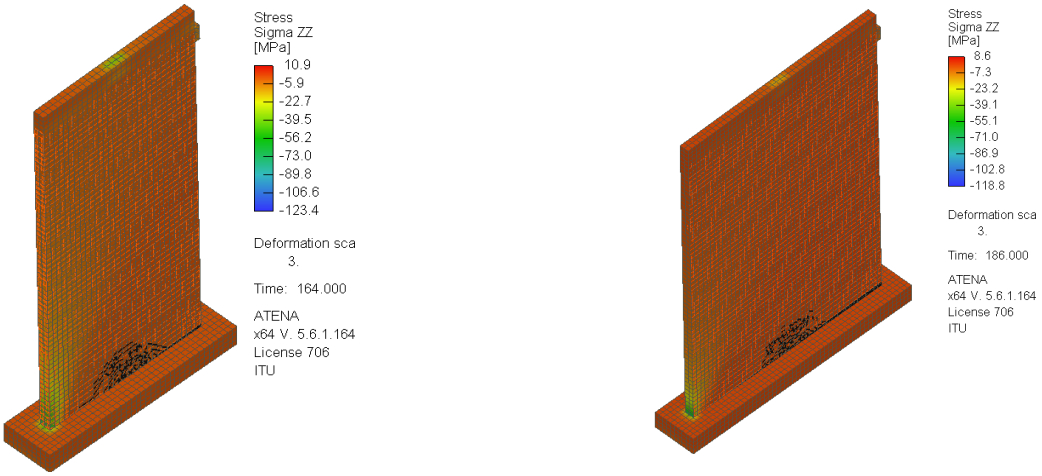

(a) (b)

Figure 11. Stress distribution: (a) W2 rocking wall system (b) W3 rocking wall system.

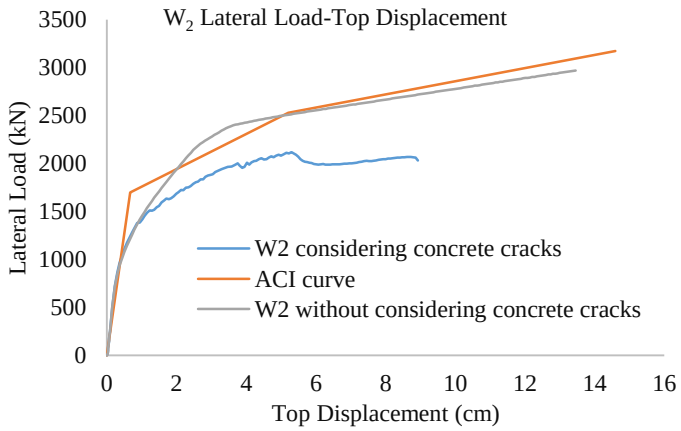

Figure 12. Lateral load-top displacement relation of W_2 rocking wall system.

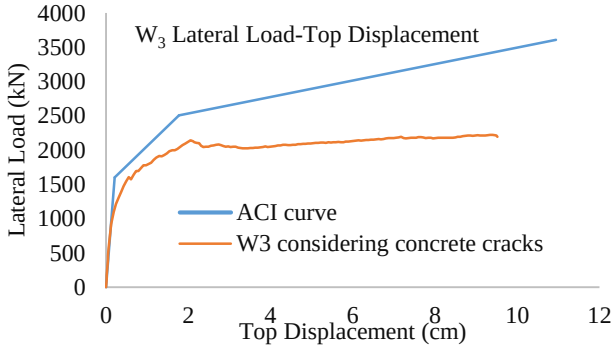

Figure 13. Lateral load-top displacement relation of W3 rocking wall system

5.3. *Coupled rocking wall system*

In this paper, two W1 single rocking walls are coupled by embedded reinforced concrete beams. Figure 14 displays the lateral load-top displacement curve of this system. Comparing to single rocking walls, the coupled system showed a better performance and higher ductility. A more detailed comparison of all systems is placed in Section 6 of this paper. The stress distribution of this system considering concrete wall and elastic wall are shown in Figure 15 (a)-(b) respectively. As it is expected in the design step, the plastic hinges are formed at both ends of coupling beams. The walls rock about their corner successfully, and the base joint model shows perfect performance. The coupled wall system shows very steady behavior before failure. The behavior of the system is investigated under realistic dead and live loads.

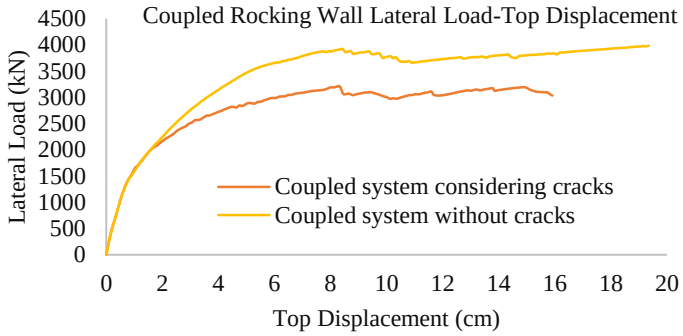

Figure 14. Lateral load-top displacement relation of coupled rocking wall systems.

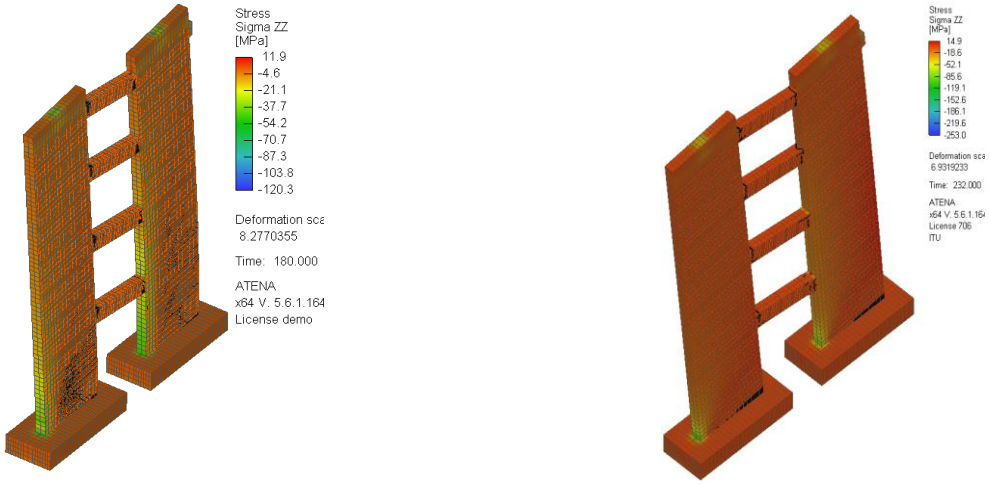

Figure 15. Stress distribution of coupled rocking wall system: (a) Considering concrete cracks in the wall panels (b) Ignoring the concrete cracks in the wall panel.

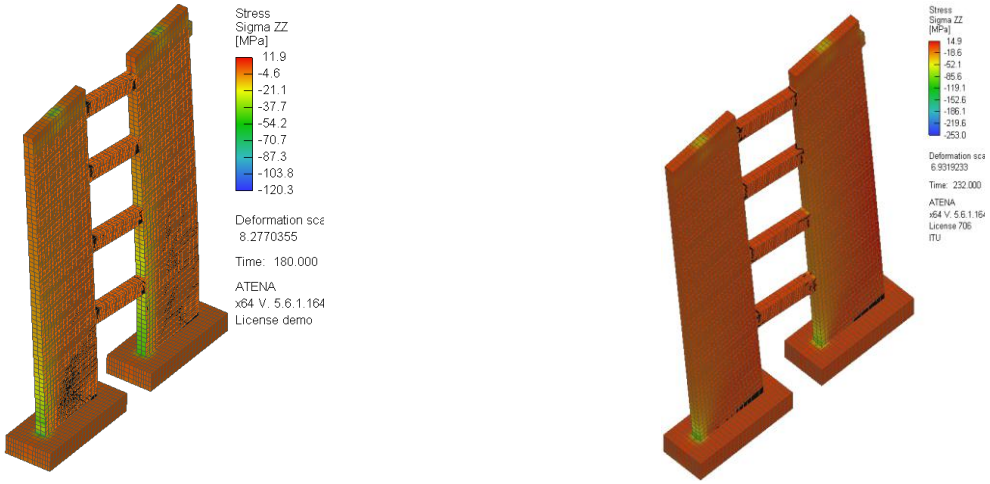

(a) (b)

Figure 16. Stress distribution of coupled rocking wall system: (a) Considering concrete cracks in the wall panels (b) Ignoring the concrete cracks in the wall panel.

5.4. *Coupled rocking wall system with end walls*

In this system, two coupled systems are connected by two end single rocking wall systems. In this study, the end walls are W_2 rocking walls. To compare the performance of different systems under lateral load, the reinforcement and post-tensioning details of each components remain unchanged. In this model, to consider the nonlinear behavior of beams, the propagation of cracks and development of plastic hinges at the end of coupling beams are allowed. However, the crack propagation at the wall panel is ignored. Figure 16 shows the stress distribution of this system. This system, the same as coupled rocking wall system, showed excellent performance. As its expected, the plastic hinges are formed at beam ends. Thanks to coupling beams, this system displayed a perfect ductility property and lateral load resisting capacity. Recent research (Nazari & Sritharan, 2020) states that despite the believe that rocking walls without additional damping devices are not dependable seismic load bearing systems, these walls engage less seismic energy and perform well with small inherent damping. Nevertheless, the study in this paper shows that coupling two rocking walls using coupled beams result in improved energy dissipation property.

The rocking action was observed throughout the end walls edge. However, monitoring the stress distribution of the system, the rocking action occurs mostly near the corner of the system, and it is reduced through the center of the end walls. The relation between the lateral load and top displacement of this system is displayed in Figure 17. To watch the performance of each panel, two monitor points, namely Point A and Point B, are chosen. It is shown in this figure that the wall panels at both sides of coupling beams show steady and similar performance with only 1 cm total displacement difference which stems from the nonlinear behavior of coupling beams and differences of gap opening at the base joints.

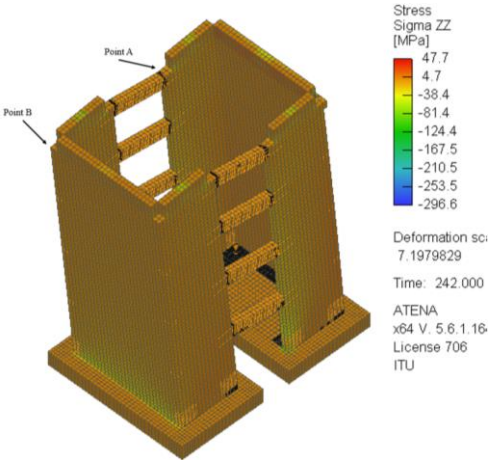

Figure 17. Stress distribution of coupled rocking wall system with end walls.

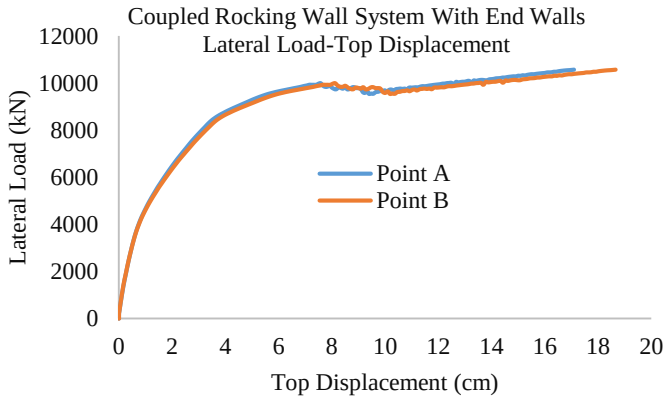

Figure 18. Lateral load-top displacement relation of coupled rocking wall system with end walls.

5.5. *Core rocking wall system*

In this system, two W_3 and two W_2 single rocking walls are combined to make a core. The stiff direction, in plan direction, of W_3 wall is towards X-direction, and that of W_2 wall is towards Y-direction. The displacement-based pushover analysis is performed in X-direction. The same as coupled systems, to have a better option of comparing different systems, the reinforcement and post-tensioning details remain unchanged. Figure 18 (a)-(b) show the stress distributions of this system under two conditions. One of which is considering the development of concrete cracks in the wall panel, and in the other case, this effect is not considered. This system shows stable performance before failure. As it is seen from Figure 18 (b), both flexural cracks in the wall panel and tensile cracks in the regions where E.D. bars are placed are formed under maximum level drift. The stress of confined concrete in the rocking toe regions are increased as high as 55 MPa.

The curve showing the relations between lateral load and top displacement of both cases are shown in Figure 19. Depending on the top displacement, the propagation of cracks in the wall panel can reduce the latera load resisting capacity of the system by approximately 30 %. It also reduces the lateral drift limit of the system significantly. It is required to note that dimensions of this system are not realistic. For a 4-story building, a core having 9.4 m × 6.28 m dimensions are too large, and the system shows extremely high initial stiffness. However, in this study these dimensions kept unchanged just to have a better understanding of the performance of different systems.

(a) (b)

Figure 19. Stress distribution of core rocking walls: (a) Ignoring the concrete cracks in the wall panel (b) Considering concrete cracks in the wall panels.

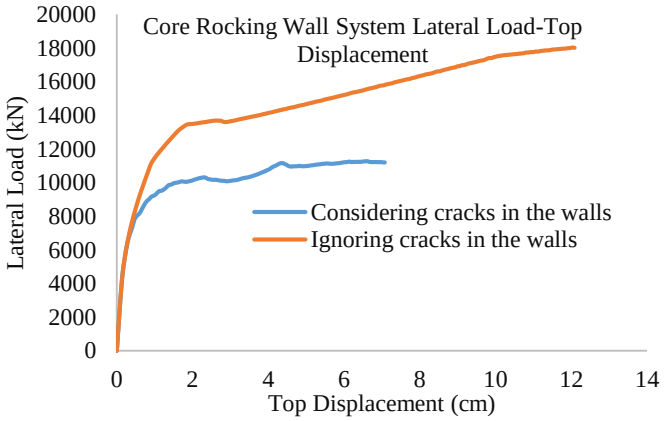

Figure 20. Lateral load-top displacement relation of core rocking wall system.

6. Conclusions

In this study, the real performance of different rocking wall systems was monitored. Two new types of these systems called core rocking wall system and coupled rocking wall system were introduced. The effect of cracks in the wall panels on the lateral load resisting capacity and lateral drift limits of these systems were studied. The lateral load-top displacement curve proposed by ACI-318 (2011) and ACI ITG-5.2 (2009) is not taking these effects into consideration. In these documents only the shear and flexural deflections are considered in estimating the lateral drift limits, and the nonlinearity in the response of rocking wall is assumed to be fully due to gap opening at the base of wall. Nevertheless, in this study, using advanced finite element analysis, we proved that effects of crack propagation on the performance of these systems should not be ignored. Depending on the system, dimensions and reinforcement details, development of cracks reduced the lateral load resisting capacity and lateral drift limits by approximately 15-20% and 25-30% respectively.

Another issue in the rocking wall systems is the spalling of concrete cover in the toe region due to cyclic loading (Henry, 2011). In this paper, section 5.1, the effect of spalling concrete of toe region on the lateral load capacity of the wall were studied numerically. It was shown that spalling of concrete cover reduces the lateral load capacity of the system by 10%. Since the spalling of concrete in toe region is not affecting much the dimension of the wall, the initial rigidity of the wall is not reduced by spalling of concrete. Comparing the stress distribution of W_1 rocking walls under two cases of having concrete cover and not having concrete cover at the region, we observed a lower stress in the second case. This is due to reduction of lateral load capacity of rocking wall.

Considering crack propagation at the base of the wall, large cracks were observed at the base of the wall near the E.D. bars. There are two main reasons behind these cracks which are the spacing of E.D. bars and there are no shear reinforcements at this region. No gap opening was observed at upper panel joints. This is specifically important in rocking wall systems. When there is a significant gap opening in the upper panel joints, the walls will rock in each story, and this will result some problems in self-centering properties of rocking walls. It is strongly recommended to design the upper join in such a way that the gap opening under design load is minimum. Additionally, the behavior of core and coupled rocking wall systems under lateral load was investigated. A comparison of the lateral load-top displacement curve of different system is shown in Figure 20.

Comparing the lateral load behavior of W_3 single rocking wall to that of coupled rocking wall system, the W_3 wall shows larger initial stiffness. The reason for this large initial stiffness is basically the large dimensions of this system. Nevertheless, the coupled system showed higher lateral load resisting capacity and excellent ductility. Larger ductility property of this system is due to formation of plastic hinges at beam ends. Coupled rocking wall systems showed a better energy dissipation property. Recently, it was stated by Nazari and Sritharan (2020) that rocking walls engage less seismic energy. This is true in terms of single rocking wall systems, but in this paper we numerically showed that coupling rocking wall using beams increases the energy dissipation of these systems.

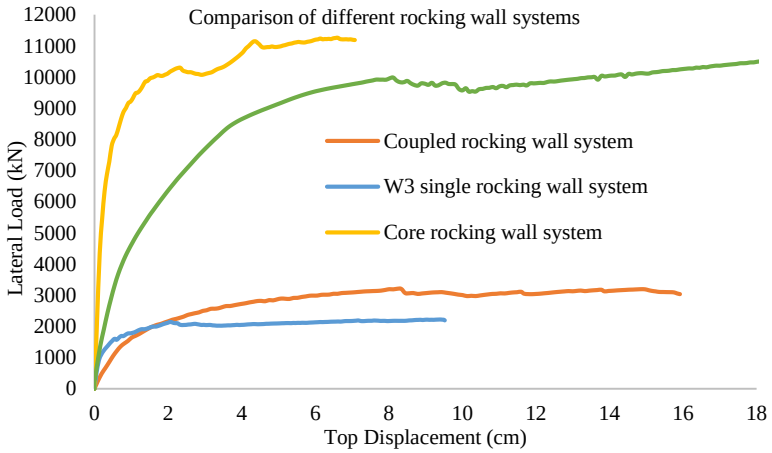

Figure 21. Lateral load-top displacement relation of various rocking wall systems.

Comparing the performance of coupled rocking wall system to coupled rocking wall system with end walls, the second system shows approximately 30 % larger lateral load resisting capacity. This results from the out of plan load bearing capacity of end walls. Both systems show excellent ductility. It is noticeable that while comparing the lateral load performance of these two systems, the fact that coupled rocking wall system with end walls include two coupled systems should be taken into consideration. Core rocking wall system showed the highest initial stiffness in contrast to all other systems. This results from large dimensions and consequently large in plan stiffness of each component. This system remains elastic till very large lateral loads. However, this rocking wall system does not show high ductility property.

In conclusion, for the high story buildings and buildings located in moderate to high seismicity regions the coupled rocking wall systems are recommended. However, for the buildings requiring small lateral drifts the core rocking walls are more favorable.

Acknowledgments: This research was financially supported by the Academic Research Project at Istanbul Technical University. The authors appreciate this support. Opinions and findings of this study are of the authors and do not necessarily reflect those of the sponsor.

References

Aaleti, S., & Sritharan, S. (2011). Performance Verification of the PreWEC Concept and Development of Seismic Design Guidelines (ISU-CCEE Report 02/11). Iowa State University. Retrieved from http://works.bepress.com/sri_sritharan/8/

ACI ITG-5.2 (2009). Requirements for Design of a Special Unbonded Post-Tensioned Precast Shear Wall Satisfying ACI ITG-5.1 and Commentary. ACI Innovation Task Group 5: Farmington Hills, MI. Retrieved from https://www.concrete.org/Portals/0/Files/PDF/Previews/ITG-5.2-09web.pdf

ACI 318 (2011). Building code requirements for structural concrete and commentary. American Concrete Institute: Farmington Hills, MI. Retrieved from https://infostore.saiglobal.com/en-us/Standards/ACI-318-2011-2625_SAIG_ACI_ACI_6467/

ASCE 7-16 (2017). Minimum Design Loads for Buildings and Other Structures. American Society of Civil Engineers: Reston, VA. Retrieved from Retrieved from https://ascelibrary.org/doi/book/10.1061/9780784414248

Aslam, M., Goddon, W. G., & Scalise, D. T. (1980). Earthquake rocking response of rigid bodies. *Journal of Structural Division, American Society of Civil Engineers*, *106*(2), 377–392. doi:10.1061/JSDEAG.0005363

ASTM A 615 (2003). *Standard Specification for Deformed and Plain Billet-Steel Bars for Concrete Reinforcement*. American Concrete Institute: Farmington Hills, MI. Retrieved from https://www.astm.org/a0615_a0615m-20.html

Červenka, V., Jendele, L., & Červenka, J. (2017). *ATENA Program Documentation, Prague*. Červenka consulting s.r.o. Retrieved from https://www.cervenka.cz/assets/files/atena-pdf/ATENA_Theory.pdf

Crippen, K. (2002). North Viaduct to Lions Gate Bridge: Vancouver engineers allow a structure to rock gently on its foundations to help it withstand a major earthquake. *Canadian Consulting Engineer*, *43*(7),34. Retrieved from https://www.canadianconsultingengineer.com/features/structures-north-viaduct-to-lions-gate-bridge/

CSI. (2018). *SAP2000 Integrated Software for Structural Analysis and Design*, Computers and Structures Inc.: Berkeley, California. Retrieved from https://www.csiamerica.com/products/sap2000

Dassault. (2011). Abaqus CAE 6.11 User's Guide, 1–1146. Retrieved from http://130.149.89.49:2080/v6.11/index.html

Egidio, A.D., Pagliaro, S., Fabrizio, C., & Leo A.M.D. (2020). Seismic performance of frame structures coupled with an external rocking wall. *Engineering Strucures, 224*(2020), 111207. doi:10.1016/j.engstruct.2020.111207

Fintel, M. (1995). Performance of buildings with shear walls in earthquakes of the last thirty years. *PCI Journal, 40*(3), 62–80. doi:10.15554/pcij.05011995.62.80

Henry, R. S. (2011). Self-centering Precast Concrete Walls for Buildings in Regions with Low to High Seismicity. Ph.D. Dissertation. University of Auckland, Auckland, New Zealand. Retrieved from http://hdl.handle.net/2292/6875

Henry, R.S., Sritharan, S. & Ingham J.M. (2016). Finite element analysis of the PreWEC self-centering concrete wall system. *Engineering Structures*, *115*, 28–41. doi:10.1016/j.engstruct.2016.02.029

Housner, G. W. (1963). The behavior of inverted pendulum structures during earthquakes. *Bulletin of the Seismological Society of America*, *53*(2), 403–417. doi:10.1017/CBO9781107415324.004

Kalliontzis, D., & Nazari, M. (2021). Unbonded Post-tensioned Precast Concrete Walls with Rocking Connections: Modeling Approaches and Impact Damping. *Frontier in Built Environment* , *7*(638509). doi:10.3389/fbuil.2021.638509

Kurama, Y. C., & Shen, Q. (2004). Posttensioned hybrid coupled walls under lateral loads. *Journal of Structural Engineering*, *130*(2), 297-309. doi:10.1061/(ASCE)0733-9445(2004)130:2(297)

Kurama, Y. C., Sause, R., Pessiki, S., Lu, L. W., & El-Sheikh, M.(1998). Seismic design and response evaluation of unbounded post-tensioned precast concrete walls (Precast Seismic Structural Systems (PRESSS) Rep. No. 98/03). Lehigh University, PA.

Kurama, Y. C., Pessiki, S., Sause, R., & Lu, L. W. (1999). Seismic behavior and design of unbonded post-tensioned precast concrete walls. *PCI Journal*, *44*(3), 72–89. doi:10.15554/pcij.05011999.72.89

Lin, C.P., Wiebe, R., & Berman, J.W. (2019). Analytical and numerical study of curved-base rocking walls. *Engineering structures*, *197*(2019), 109397. doi:10.1016/j.engstruct.2019.109397

Moroder, D., Sarti, F., Palermo, A., & Pampanin, S. (2014). Experimental investigation of wall-to-floor connections in post-tensioned timber buildings: *Proceeding of the towards integrated seismic design conference*. Auckland. Retrieved from http://db.nzsee.org.nz/2014/poster/25_Moroder.pdf

Nazari, M., & Sritharan, S. (2020). Influence of different damping components on dynamic response of concrete rocking walls. *Engineering Structure*, *212*(2020), 110468. doi:10.1016/j.engstruct.2020.110468

Prakash, G.H. Powell (1993). *DRAIN-2DX-Version 1.02 – User Guide* (Report No. UCB/SEMM-93/17). Civil Eng. Dept., University of California at Berkeley, CA. Retrieved from https://nisee.berkeley.edu/elibrary/semm/1993

Priestley, M. J. N. (1991). Overview of PRESSS research program. *PCI Journal*, *36*(4), 50–57. doi:10.15554/pcij.07011991.50.57

Priestley, M. J. N., Sritharan, S. S., Conley, J. R., & Pampanin, S. (1999). Preliminary results and conclusions from the PRESSS five-story precast concrete test building. *PCI Journal*, *44*(6), 42–67. doi:10.15554/pcij.11011999.42.67

Sritharan, S., Aaleti S., Henry R.S., Liu K.Y. & Tsai K.C. (2015). Precast concrete wall with end columns (PreWEC) for earthquake resistant design. *Earthquake Engineering and Structural Dynamics , 44* (12), 2075 2092. doi:10.1002/eqe.2576

Smith, B. J., & Kurama, Y. C. (2012). Seismic Design Guidelines for Special Hybrid Precast Concrete Shear Walls (Structural Engineering Research Report NDSE-2012-02). University of Notre Dame.

Stone, W. C., Cheok, G. S., & Stanton, J. F. (1995). Performance of Hybrid Moment-Resisting Precast Beam-Column Concrete Connections Subjected to Cyclic Loading. *ACI Structural Journal*, *91*(2), 229-249. doi: 10.14359/1145

Vayas, I., Dasiou, M. E., & Marinelli, A. (2007). Säulen Griechischer Tempel Unter Erdbebenbeanspruchung. *Bautechnik*, *84*(6), 388–396. doi:10.1002/bate.200710034

Watkins, J., Sritharan, S., & Henry, R.S. (2014). An Experimental Investigation of a Wall-to-Floor Connector for Self-Centering Walls: *Proceeding of the 10th U.S. National Conference on Earthquake Engineering*. Anchorage, Alaska. doi:10.4231/D3BZ61862